Sinopfbd, 2026; 11(1): 219-242 https://doi.org/10.33484/sinopfbd.1767947

Sinop Üniversitesi Fen Bilimleri Dergisi
Sinop Uni J Nat Sci

E-ISSN: 2564-7873

https://dergipark.org.tr/tr/pub/sinopfbd

Structural Evaluation of the February 6, 2023 Türkiye Earthquakes: Comparison of Design Codes and Recorded Seismic Demands

Eray OZKAN

How to cite: Ozkan, E. (2026). Structural evaluation of the February 6th, 2023 Türkiye earthquakes: Comparison of design codes and recorded seismic demands. *Sinop Üniversitesi Fen Bilimleri Dergisi, 11*(1), 219-242. https://doi.org/10.33484/sinopfbd.1767947

Open Access

Research Article

Corresponding Author
Eray OZKAN
eray.ozkan@cbu.edu.tr

ORCID of the Author
E.O: 0000-0003-4755-8207

Received: 07.08.2025
Accepted: 06.03.2026

Abstract

Türkiye witnessed devastating earthquakes on February 6, 2023, causing widespread destruction across a wide region. In this study, the seismic impact of these events is evaluated from a structural design perspective. Specifically, the recorded Peak Ground Acceleration (PGA) values and response spectra are presented together with the elastic design acceleration parameters and design spectra prescribed in historical and current building codes. The results revealed that the ground motions experienced in the region may correspond to the highest acceleration values ever recorded. Results show that these findings may contain valuable information for refining Probabilistic Seismic Hazard Analysis (PSHA) and Ground Motion Prediction Equations (GMPEs). Since these methods rely heavily on historical seismicity and empirical strong motion data, the documentation of such extreme intensities provides a critical basis for recalibrating future hazard assessments and revising structural design parameters specified in building regulations.

Keywords: Earthquake, equivalent earthquake load, earthquake spectra, RC residential buildings, earthquake code

6 Şubat 2023 Türkiye Depremlerinin Yapısal Değerlendirmesi: Tasarım Yönetmelikleri ile Kaydedilen Sismik Taleplerin Karşılaştırılması

Manisa Celal Bayar University, Manisa Vocational School of Technical Sciences, Construction Department, Manisa, 45140, Türkiye

Özet

Türkiye, 6 Şubat 2023 tarihinde geniş bir bölgede yaygın yapısal hasarlara neden olan yıkıcı depremlere sahne olmuştur. Bu çalışmada, söz konusu olayların sismik etkileri yapısal tasarım perspektifinden değerlendirilmiştir. Özellikle, kaydedilen En Büyük Yer İvmesi (PGA) değerleri ve tepki spektrumları; geçmiş ve yürürlükteki bina yönetmeliklerinde öngörülen elastik tasarım ivme parametreleri ve tasarım spektrumları ile birlikte sunulmuştur. Sonuçlar, bölgede yaşanan yer hareketlerinde oluşan ivmelerin, bugüne kadar kaydedilen en yüksek ivme değerlerine karşılık gelebileceğini ortaya koymuştur. Elde edilen bu bulgular, Olasılıksal Sismik Tehlike Analizi (PSHA) ve Yer Hareketi Tahmin Denklemlerinin (GMPE) iyileştirilmesi adına değerli bilgiler içermektedir. Bu yöntemler büyük ölçüde tarihsel sismisiteye ve ampirik yer hareketi verilerine dayandığından; bu denli sıra dışı düzeydeki yer hareketlerinin belgelenmesi, gelecekteki tehlike değerlendirmelerinin yeniden kalibre edilmesi ve bina yönetmeliklerinde belirtilen yapısal tasarım parametrelerinin revize edilmesi için kritik bir temel oluşturmaktadır.

Anahtar Kelimeler: Deprem, eşdeğer deprem yükü, deprem spektrumları, BA konut binaları, deprem yönetmeliği

Introduction

Türkiye is located in one of the world's most active seismic zones -the Alpine-Himalayan Belt- and has confronted numerous earthquakes throughout its history, resulting in significant damage to thousands of structures. Evaluating the seismic resilience of structures, understanding seismic risks, and designing safer buildings are among the primary responsibilities of the engineering community. From this perspective, the earthquakes of February 6, 2023, should serve as a turning point for understanding Türkiye's seismic risk profile, examining structural deficiencies, and assessing structural design parameters. Across the entire country, 140 ground motions ranging in magnitude (M_W) from 3.9 to 7.7 occurred in a single day. Additionally, within the three months up to May 6, a total of 33,591 ground motions, with magnitudes up to 6.6 (M_W) were recorded in Kahramanmaraş and its surrounding areas. According to official reports, the earthquakes resulted in the loss of 50.783 lives, with 115.353 injuries, and led to the collapse of 37.984 buildings [1]. Over the course of more than three years, many researchers have examined the February 6 earthquakes and their effects and contributing to the literature on the causes of earthquake effects. A significant part of the work carried out consists of determining the structural damage to reinforced concrete structures following earthquakes in the region [2-8]. In these studies, various causes of building collapse have emerged, as summarized in Table 1. Construction errors are often prominent among the cited reasons in these studies, while inadequacies in the design have also come to light.

Table 1. *Collapse reasons of reinforced concrete buildings on February 6*

Category	**Reason of collapse**	**Study**						
		İnce [2]	Öztürk et al. [3]	Altunsu et al. [4]	Ivanov & Chow [5]	Yıldız & Kına [6]	Binici et al. [7]	Peker & Altan [8]
Construction	Reinforcement and stirrup placement error	X	X	X	X	X		X
Outdated Practice	Faulty manufacturing before the year 2000		X	X	X	X	X	X
Design	Insufficient shear walls	X	X	X		X	X	
Construction	Insufficient concrete strength	X	X		X			X
Outdated Practice	Strong beam / weak column structure	X	X	X		X		
Construction	Inadequate gaps between adjacent buildings	X		X		X		X
Design	Hollow, thin or non-rigid slab	X	X		X		X	
Design	Insufficient soil parameters or incorrect evaluation of soil parameters	X	X				X	
Design	Building irregularities (soft storey, short column, weak storey etc.)	X	X					X
Ground motion	Earthquake demands higher than design values		X	X			X	
Construction	Stair connections and reinforcement errors in stairs	X				X		
Usage	Damage to structural elements as a result of unconscious use		X	X				
Construction	Labor mistakes					X	X	
Design	Rigid infill wall connections	X						
Design	Faulty and incomplete strengthening applications		X					
Design	Inappropriate structural and architectural projects in terms of earthquake engineering		X					

While construction regulations have been continually updated over the years, disasters have pushed authorities to pursue safer buildings, and the Marmara (M_W 7.6) and Düzce (M_W 7.2) earthquakes in

1999 created a domino effect for the construction industry in the country. Many practices came into force after these disasters. In some of these, in-situ concrete production has been prohibited since 2000, and the use of ready-mixed concrete in accordance with the standards has been stipulated. Building inspection practice began in 2001. Before this date, there was no inspection during the construction phases of residential buildings. In the same year, the use of round bars in concrete reinforcement was prohibited, and in 2002, a standard for ready-mixed concrete was issued, making it compulsory in 2004. As a result of these important changes, particularly affecting construction materials, the year 2000 has become a milestone for building construction in Türkiye. Indeed, field investigations following the February 6 earthquakes consistently highlighted the severe vulnerability of structurally deficient buildings constructed prior to 2000. Additionally, studies have shown that more robust structures can be built using simple improvement methods such as shear walls or sliding control mechanisms [7]. In some studies, the classification of the damage observed in the field was evaluated [8-10], and studies were carried out on masonry structure damage [9, 11] and on the existing building stock [10, 12]. On the other hand, there are also studies examining earthquake-soil interaction [13], near-fault effects [14], and earthquake characteristics [15-17]. In addition to the studies related to the earthquake characteristics and damage detection, recorded ground accelerations have also been examined in some studies [2, 3, 6, 8, 18]. However, these recorded accelerations were generally not compared against the design limits prescribed by the codes. Furthermore, most studies reported only the peak ground acceleration (PGA) values, neglecting the vector resultants of these accelerations. On the other hand, evaluations in all of the studies were based on the magnitude of earthquakes, so only the effects of the Pazarcık (M_W 7.7) and Elbistan (M_W 7.6) earthquakes and the spectra associated with the two were examined. The concept of earthquake magnitude serves as a measure of the force required to generate the observed seismic waves and is fundamentally related to the released seismic energy [19]. In construction design, however, the considered horizontal ground motion demand is proportional to the acceleration directly transmitted to the structure, and is derived from the inertia force of Newton's law of motion. In other words, while earthquakes are evaluated according to their magnitude in other disciplines, the determining factor in building design is the accelerations transmitted by earthquakes to the building. This study aims to evaluate the ground accelerations caused by the earthquakes that occurred on February 6, 2023. In the evaluation, the design conditions in the codes and the earthquake demand were presented. Therefore, the main contribution of this study is not to develop a new analytical method or theoretical model. Instead, it focuses on the systematic analysis and interpretation of the recorded ground accelerations and corresponding response spectra from the February 6 earthquakes. To provide a broader context for international readers, the observed seismic demands are also evaluated in light of prominent global seismic provisions. The lessons learned from the February 6 earthquakes are surely expected to contribute to efforts of regulation studies and probabilistic seismic risk assessment studies in earthquake-prone areas.

Materials and Methods

Design Earthquake Load

Historical seismic events have underscored the critical importance of earthquake-resistant design within the national construction industry. After the 1939 Erzincan (M_W 7.8) Earthquake, various earthquake regulations began to be implemented in order to make the structures built in Türkiye resistant to earthquake effects. With the first code that came into force, the earthquake load that would affect the building was obtained by multiplying the weight of the building by a certain coefficient, and it was accepted that this load acted as a single base shear load representing the entire earthquake effects. Later on, the design earthquake load calculation was revised by taking into account factors such as soil type and building importance coefficients; it was named Equivalent Earthquake Load with the 1998 code and was also used in the earthquake codes released in 2007 and 2018 [20]. In this section, first, the earthquake loads in the codes used for design are examined. Considering the existing building stock, earthquake loads are obtained for residential buildings with reinforced concrete frame bearing systems in the codes of 1975 and later. Afterwards, the seismic demands of the February 6 earthquakes are presented. In the design earthquake load calculations, an effort was made to determine the highest inertial demand that could be obtained acting on most of the buildings. The aim is to obtain the design loads considered in the design of the majority of existing residential building stock. To achieve a comprehensive evaluation, a conservative upper-bound approach was adopted. For parameters dependent on the natural vibration period, it was assumed that the building's period falls within the constant acceleration plateau, thereby maximizing the spectral coefficient. Similarly, coefficients for high ductility reinforced concrete frames were used for structural behavior, as this is the design target for typical residential buildings in the region.

Static Equivalent Horizontal Load (TEC-1975)

The Code on Structures to be Built in Disaster Areas [21] contains similarities with today's modern regulations. Dimensions and rebar details for reinforced concrete elements are given, and Türkiye is divided into five different earthquake zones (Figure 1).

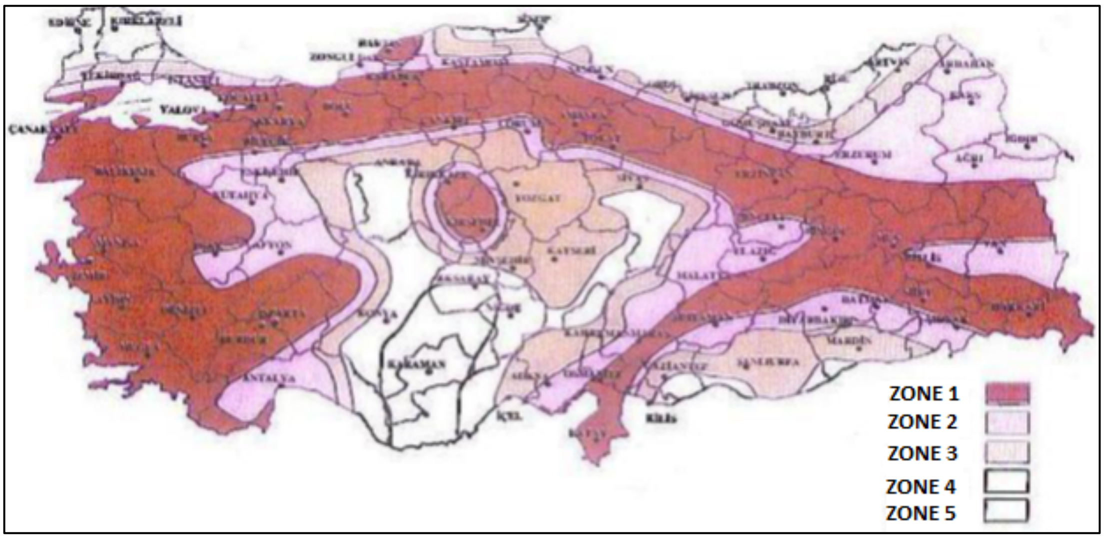

Figure 1. *Earthquake hazard map - 1972 [21]*

In the code, the Static Equivalent Horizontal Load to be used in dimensioning of earthquake-resistant buildings is calculated with the following equations.

$$F = C\,W \tag{1}$$

$$C = C_0\,K\,S\,I \tag{2}$$

$$S = \frac{1}{|0{,}8 + T - T_0|} \tag{3}$$

In Equations (1), (2), and (3), F is defined as the Static Equivalent Horizontal Load, W is the weight of the building, C is the Earthquake Coefficient, C_0 is the Earthquake Zone Coefficient, K is the Building Type Coefficient, S is the Building Dynamic Coefficient, and I is the Building Importance Factor. Since the maximum value of 1.0 is given for the S value in the code, S = 1.0 was taken to obtain the highest load value, and the C_0 value was taken as 0.1 for earthquake zone 1. The earthquake load was then calculated by taking the K coefficient as 1.0 for ductile frames with unreinforced masonry partition walls and I = 1.0 for residential buildings. Thus, the C coefficient was obtained as 0.1, and F = 0.1 W.

Equivalent Earthquake Load in TEC-1998 and TEC-2007

With every earthquake that occurs, the earthquake performance of buildings is also questioned. After the 1995 Kobe Earthquake (M_W 6.9), the earthquake hazard map was revised in Türkiye. Building irregularities were defined for the first time in the Regulation on Structures to be Built in Disaster Areas [22] published in 1998, and effective ground acceleration coefficient and design spectrum coefficients were added in the horizontal earthquake load calculation. The calculated base shear force was named as Equivalent Earthquake Load, and this method continued to be used with the Regulation on Buildings to be Constructed in Earthquake Zones [23], which came into force in 2007. Another two methods, Mode Combination and Time History Analysis, were the alternatives, and the usage areas of the Equivalent Earthquake Load method were limited in both codes (Table 2).

Table 2. *Building designs where the Equivalent Earthquake Load method can be applied [22, 23]*

Eq. Zone	Building Type	Total Height Limit (TEC-1998)	Total Height Limit (TEC-2007)
1 and 2	Buildings that meet the condition of torsional irregularity below 2 at each storey ($\eta bi \leq 2.0$)	$H_N \leq 25$ m	$H_N \leq 25$ m
1 and 2	Buildings that meet the condition of torsional irregularity below 2 at each storey ($\eta bi \leq 2.0$) and without type B2 irregularity	$H_N \leq 60$ m	$H_N \leq 40$ m
3 and 4	All buildings	$H_N \leq 75$ m	$H_N \leq 40$ m

The Equivalent Earthquake Load calculation, which was determined by the code published in 1998, was not changed by the code published in 2007, but was used exactly as it was. The formulas used are given below.

$$V_t = \frac{WA(T_1)}{R_a(T_1)} \geq 0.1\, A_0\, I\, W \quad (4)$$

In Equation 4, V_t is the total Equivalent Earthquake Load, W is the Building Weight, $A(T_1)$ is the Spectral Acceleration Coefficient, $R_a(T_1)$ is the Earthquake Load Reduction Coefficient, T_1 is the first period of the building, A_0 is the Effective Ground Acceleration Coefficient, and I is the Building Importance Factor. Spectral Acceleration Coefficient $A(T_1)$ can be calculated with Equation 5.

$$A(T_1) = A_0\, I\, S(T_1) \quad (5)$$

S(T) is defined as the Spectrum Coefficient and is calculated with the following equations depending on the building's natural period T ($S(T_1)$ for the first period) and the Spectrum Characteristic Periods T_A and T_B.

$$S(T) = 1 + 1.5\frac{T}{T_A} \qquad (0 \leq T \leq T_A) \quad (6)$$

$$S(T) = 2.5 \qquad (T_A \leq T \leq T_B) \quad (7)$$

$$S(T) = 2.5\left(\frac{T_B}{T}\right)^{0,8} \qquad (T_B \leq T) \quad (8)$$

T is the building's natural period, Spectrum Characteristic Periods T_A and T_B in the Equations (6), (7), and (8) are determined depending on the Local Soil Classes. Since the base shear force will be calculated in the most unfavorable condition within the scope of this study, it is accepted that the natural period of the designed building is within the Spectrum Characteristic Periods T_A and T_B value range. Thus, the S(T) Spectrum Coefficient was obtained as 2.5. The Seismic Load Reduction Coefficient $R_a(T)$ was determined depending on R (Structural Behavior Factor) and the natural vibration period T.

$$R_a(T) = 1.5 + (R - 1.5)\frac{T}{T_A} \qquad (0 \leq T \leq T_A) \quad (9)$$

$$R_a(T) = R \qquad (T_A < T) \quad (10)$$

where $R_a(T)$ is the Seismic Load Reduction Coefficient, R is the Structural Behavior Factor, T is the building's natural period and T_A and T_B are Spectrum Characteristic Periods. For the earthquake load to be calculated in this study, Equation 10 was used since it is assumed that the natural period of the building is within the T_A and T_B range. Thus, by obtaining R = 8 from the relevant table for buildings with high ductility, and all earthquake loads carried by frames, the Seismic Load Reduction Coefficient ($R_a(T)$) was obtained as 8.0. Among the other parameters, the Building Importance Coefficient is 1.0 for residential buildings and the Effective Ground Acceleration Coefficient (A_0) was taken as 0.4 for the first earthquake zone (Figure 2). Thus, $V_t = 0.125$ W was found.

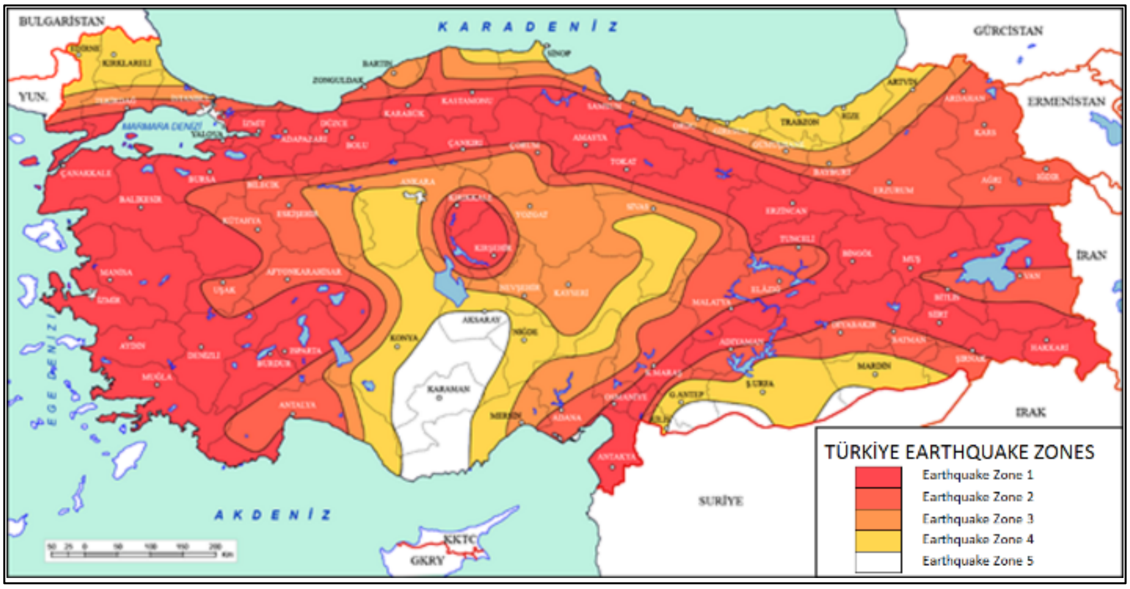

Figure 2. *Türkiye earthquake hazard map - 1996 [24]*

Equivalent Earthquake Load in TBEC-2018

The Türkiye Building Earthquake Code [25] came into force in 2019 with many changes in structural design. With the complete removal of earthquake zones, the spectral data to be used in design can be obtained depending on the location on the earthquake hazard map, allowing the design of buildings according to more than one performance target. In addition, the building usage classes were revised, and building height classes were added in the calculations. The Equivalent Earthquake Load method was taken its place among the linear calculation methods that can be used within the scope of Design by Strength, but as in the previous two specifications, the use of the method is still limited. The limit conditions were determined according to torsional irregularity, Building Height Class (BHC) and Earthquake Hazard Class (EHC) parameters (Table 3).

Table 3. *Building designs where the Equivalent Earthquake Load method can be applied [25]*

Building Type	**Permissible Building Height Class**	
	EHC=1, 1a, 2, 2a	EHC=2, 2a, 4, 4a
Buildings that meet the condition of torsional irregularity below 2 at each storey ($\eta bi \leq 2.0$) and without type B2 irregularity	BHC $\geq$ 4	BHC $\geq$ 5
All other buildings	BHC $\geq$ 5	BHC $\geq$ 6

Within the limitations given in Table 3, the total Equivalent Earthquake Load $V_{tE}(X)$ (base shear force) acting on the entire building in the "X" direction taken into account for reinforced concrete residential buildings is calculated according to the formula below.

$$V_{tE}^{(X)} = m_t\, S_{aR}\left(T_p^{(X)}\right) \geq 0.004\, m_t\, I\, S_{DS}\, g \quad (11)$$

In Equation 11, m_t represents the total mass of the building, and $S_{aR}(T_p(X))$ represents the Reduced Design Spectral Acceleration determined for the dominant natural vibration period of the building ($T_p(X)$). The $V_{tE}(X)$ value is subject to a minimum threshold defined by the Building Importance Factor (I), the Design Spectral Acceleration Coefficient for short periods (S_{DS}), and the gravitational acceleration (g).

$$S_{aR}(T) = \frac{S_{ae}(T)}{R_a(T)} \quad (12)$$

The Reduced Design Spectral Acceleration $S_{aR}(T)$ is derived from the Horizontal Elastic Design Spectral Acceleration ($S_{ae}(T)$) calculated for the DD-2 earthquake ground motion level, divided by the Earthquake Load Reduction Coefficient $R_a(T)$ (Equation 12). As illustrated in the design response spectrum (Figure 3), the corner periods T_A and T_B are functions of the spectral parameters S_{DS} and S_{D1}. To capture the most critical seismic demand, $S_{ae}(T)$ was taken as equal to S_{DS} by assuming that the building's period falls within the plateau range between T_A and T_B.

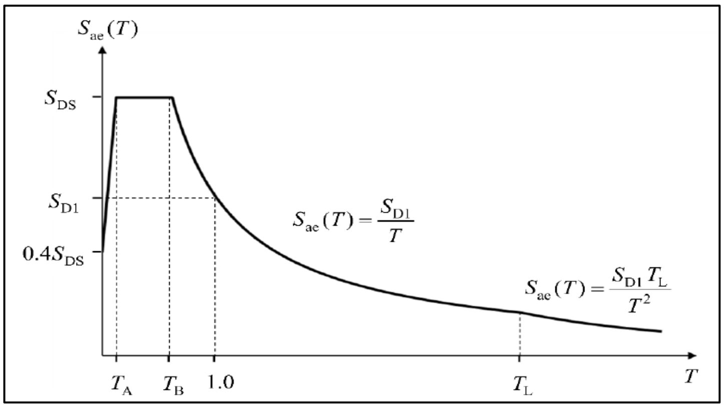

Figure 3. *Horizontal elastic design spectrum [25]*

In accordance with the assumption that the building's natural period falls within the plateau of the design spectrum ($T_A<T<T_B$), the Seismic Load Reduction Coefficient $R_a(T)$ is determined as per Equation 13. This coefficient is fundamental for scaling down the Horizontal Elastic Design Spectral Acceleration ($S_{ae}(T)$) to account for the structure's ductility and overstrength.

$$R_a(T) = D + \left(\frac{R}{I} - D\right)\frac{T}{T_B} \qquad T \leq T_B \quad (13)$$

Here, R denotes the Structural Response Coefficient (Response Modification Factor), D represents the Strength Excess Factor, I is the Building Importance Factor, T represents the natural vibration period of the building, and T_B represents the spectrum corner period. In this study, in order to evaluate the highest possible shear force, the lowest possible $R_a(T)$ was targeted by setting $T = T_B$ consistent with the assumption used for $S_{ae}(T)$. Thus, $R_a(T)$ simplifies to R/I. For the reinforced concrete frame residential buildings with high ductility considered in this study, R = 8.0 and I = 1.0, resulting in $R_a(T) = 8.0$. Consequently, the Reduced Design Spectral Acceleration is defined as $S_{aR}(T) = S_{DS}/8.0$. The Short-Period Design Spectral Acceleration Coefficient (S_{DS}), a critical parameter for defining the spectral plateau, is derived from map-based spectral values adjusted by site-specific soil coefficients. In the context of the analysis, the S_{DS} value was obtained from the Türkiye Earthquake Hazard Map at the coordinates of AFAD Station 4614, where there extreme demands were recorded during the February 6 Pazarcık Earthquake with a magnitude of M_W 7.7. The S_{DS} value, in accordance with the ZC soil classification of the station, was calculated to be 1.352 g. Consequently, the final design parameters were calculated as $S_{aR}(T) = 0.169$ g and the total base shear value as $V_{tE} = 0.169$ W.

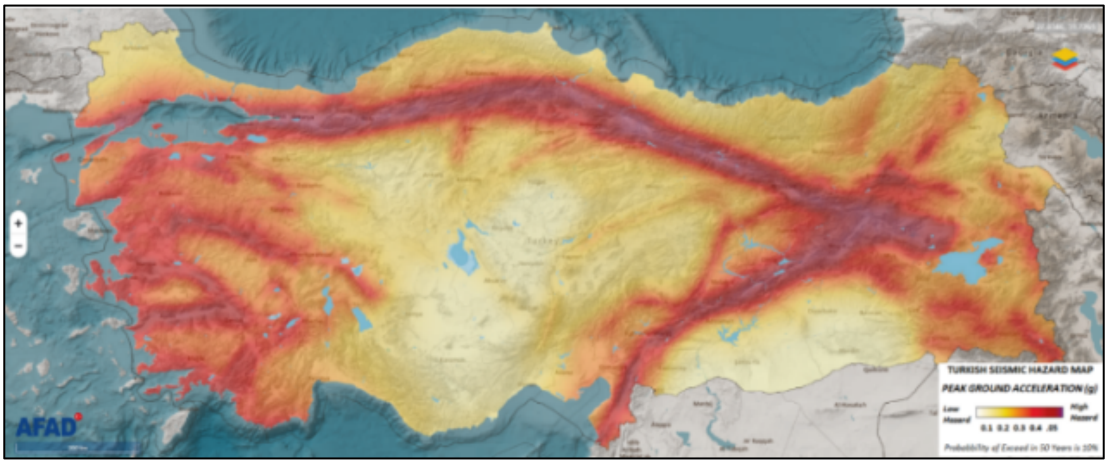

Figure 4. *2018 Türkiye earthquake hazard map [26]*

The calculation parameters and assumptions adopted to determine the Equivalent Earthquake Loads across different regulatory periods are summarized in Table 4. In the present comparative analysis, the "conservative upper-bound" approach was strictly followed to determine the maximum base shear force prescribed by the codes. In this regard, the natural vibration period (T) was assumed to lie within the plateau of the characteristic spectrum ($T_A \leq T \leq T_B$) where the Horizontal Elastic Design Spectral Acceleration ($S_{ae}(T)$) takes its maximum value (S_{DS}). This assumption was followed in accordance with the inherent dynamic characteristics of the low to mid-rise Reinforced Concrete Buildings, which form a major portion of the building stock of the region. The extension of this assumption to the general building stock, including low-rise buildings, was justified by the inherent phenomenon of stiffness degradation and period extension. In the presence of strong ground motions, the Reinforced Concrete members crack and yield, resulting in a significant extension of the fundamental period of the structure. Consequently, considering the multitude of high-intensity seismic events evaluated, basing the calculations on this plateau provides a representative critical demand envelope for a significant portion of the building stock affected by the earthquakes.

Table 4. *Summary of parameters used for Design Earthquake Load calculation across codes*

Code / Parameter	TEC-1975	TEC-1998 & TEC-2007	TBEC-2018	Justification
Zone / Hazard Map Loc.	Zone 1 (C_0 = 0.10)	Zone 1 (A_0 = 0.40)	SDS = 1.352 (Station 4614)	Highest hazard zone assumptions.
Building Type	RC Frame	RC Frame	RC Frame	Typical building stock.
Importance Factor (I)	1	1	1	Residential buildings.
Structural Behavior	Ductile Frame (K = 1.0)	High Ductility (R = 8)	High Ductility (R = 8)	Frame structure.
Soil / Period Assumption	S = 1.0 (Max value)	$T_A \leq T \leq T_B$ (Plateau)	$T_A \leq T \leq T_B$ (Plateau)	Assumed "plateau" range to yield max. spectral acceleration.
Resulting Load Formula	F = 0.10 W	V_t = 0.125 W	V_{tE} = 0.169 W	Base shear force relative to weight.

Ground Motion Demands on February 6

A total of 138 ground motions were recorded in Kahramanmaraş and surrounding provinces on February 6, 2023, and 25 of these records had magnitudes of 5.0 or above. The locations of the events that occur are shown in Figure 5, with their sizes and colors varying according to their magnitude [27].

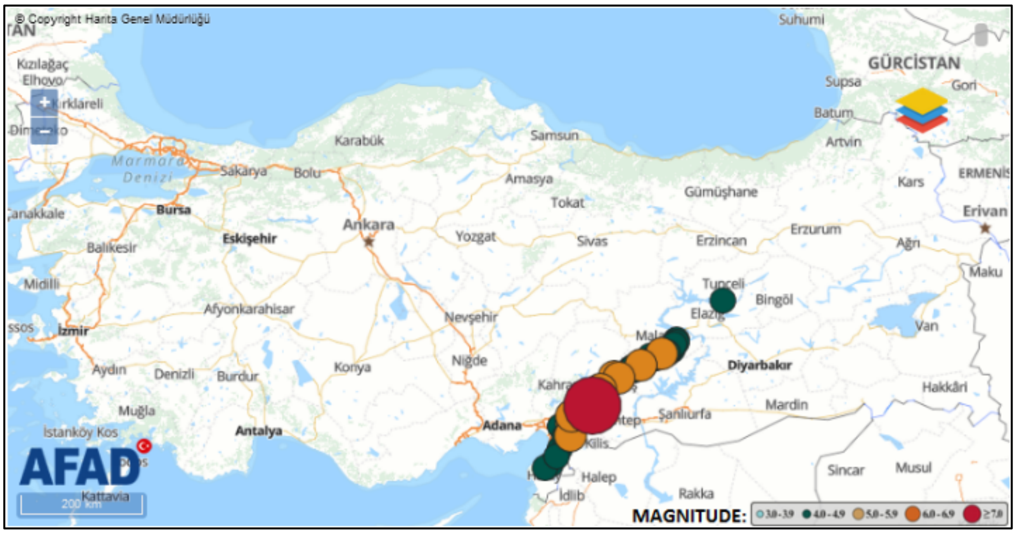

Figure 5. *Ground motions on February 6, 2023 [27]*

Ground motions with magnitudes of 5.0 and above are given in Table 5. The ground acceleration data recorded at the stations during these earthquakes, including the recorded peak ground acceleration (PGA) values were obtained from the AFAD database [27].

Table 5. *Ground motion event list in 06.02.2023 [27]*

Event ID	Date/Time (Local)	Magnitude	Type	Depth (km)	Location	PGA (g)
543428	06.02.2023 04:17	7.7	M_W	8.60	Pazarcık (Kahramanmaraş)	2.22
543429	06.02.2023 04:26	5.6	M_L	6.98	Nurdağı (Gaziantep)	0.05
543431	06.02.2023 04:28	6.6	M_W	6.20	Nurdağı (Gaziantep)	0.46
543430	06.02.2023 04:36	5.7	M_L	11.19	İslahiye (Gaziantep)	0.37
543438	06.02.2023 04:51	5.0	M_W	7.00	İslahiye (Gaziantep)	0.14
543442	06.02.2023 04:51	5.3	M_W	6.63	İslahiye (Gaziantep)	0.14
543433	06.02.2023 04:58	5.3	M_W	10.21	İslahiye (Gaziantep)	0.16
543437	06.02.2023 05:00	5.3	M_W	7.00	Gölbaşı (Adıyaman)	0.04
543434	06.02.2023 05:01	5.3	M_W	16.44	Pazarcık (Kahramanmaraş)	0.02
543439	06.02.2023 05:03	5.6	M_W	10.23	Doğanşehir (Malatya)	0.05
543447	06.02.2023 05:06	5.1	M_W	6.95	Çelikhan (Adıyaman)	0.08
543436	06.02.2023 05:23	5.3	M_W	11.81	Nurdağı (Gaziantep)	0.09
543531	06.02.2023 09:54	5.0	M_W	7.00	Çağlayancerit (Kahramanmaraş)	0.01
543593	06.02.2023 13:24	7.6	M_W	7.00	Elbistan (Kahramanmaraş)	0.65
565451	06.02.2023 13:26	5.8	M_L	6.89	Yeşilyurt (Malatya)	0.21
543595	06.02.2023 13:32	5.5	M_L	10.93	Ekinözü (Kahramanmaraş)	0.08
543636	06.02.2023 16:17	5.2	M_W	3.94	Göksun (Kahramanmaraş)	0.05
543638	06.02.2023 16:39	5.3	M_W	7.20	Doğanşehir (Malatya)	0.02
543639	06.02.2023 16:44	5.1	M_W	8.76	Nurhak (Kahramanmaraş)	0.04
543664	06.02.2023 18:14	5.0	M_W	7.04	Doğanşehir (Malatya)	0.43
543669	06.02.2023 18:33	5.3	M_W	11.15	Yeşilyurt (Malatya)	0.02
543718	06.02.2023 21:03	5.2	M_W	12.79	Göksun (Kahramanmaraş)	0.01
543721	06.02.2023 21:05	5.0	M_W	7.03	Göksun (Kahramanmaraş)	0.01
543773	06.02.2023 23:37	5.5	M_W	5.96	Pazarcık (Kahramanmaraş)	0.05
543774	06.02.2023 23:40	5.2	M_W	5.82	Yeşilyurt (Malatya)	0.01

Pazarcık Earthquake (7.7 M_W)

The Pazarcık (Kahramanmaraş) Earthquake was the first of the seismic sequence that occurred in the region on February 6, 2023 at 04:17 (local time) on the Eastern Anatolian fault line with a magnitude of M_W 7.7, in the Pazarcık district of Kahramanmaraş. The ground motions caused by the earthquake were felt all over the country, except the Marmara and Aegean Regions, and recorded at a total of 361 observation stations (Figure 6).

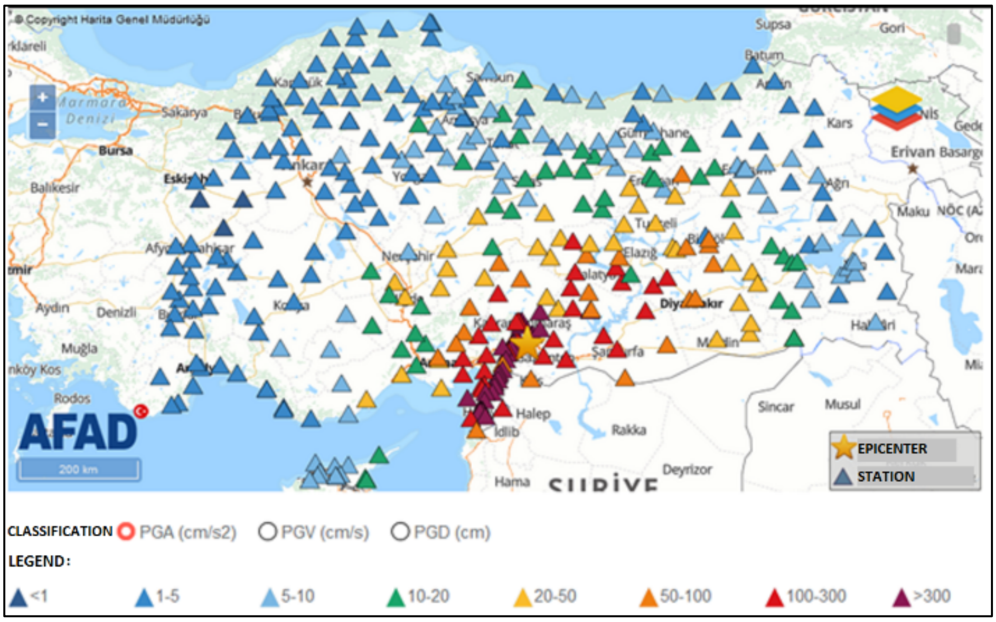

Figure 6. *Acceleration records of the Pazarcık Earthquake (7.7 M_W) [27]*

The highest ground motion intensities were recorded at station 4614. This station is located at Pazarcık Regional School (37.48513˚ N, 37.29775˚ E, altitude of 771 m), which is classified as ZC site class with a V_{s30} value of 541 m/s [27]. The acceleration time-history records were obtained in three orthogonal directions (EW, NS, and UD). Upon analysis of these records, the Peak Ground Acceleration (PGA) values were identified as 2.22 g in the East-West direction, 2.21 g in the North-South direction, and 1.99 g in the Up-Down direction. Figure 7 illustrates the superimposed acceleration traces for all directions.

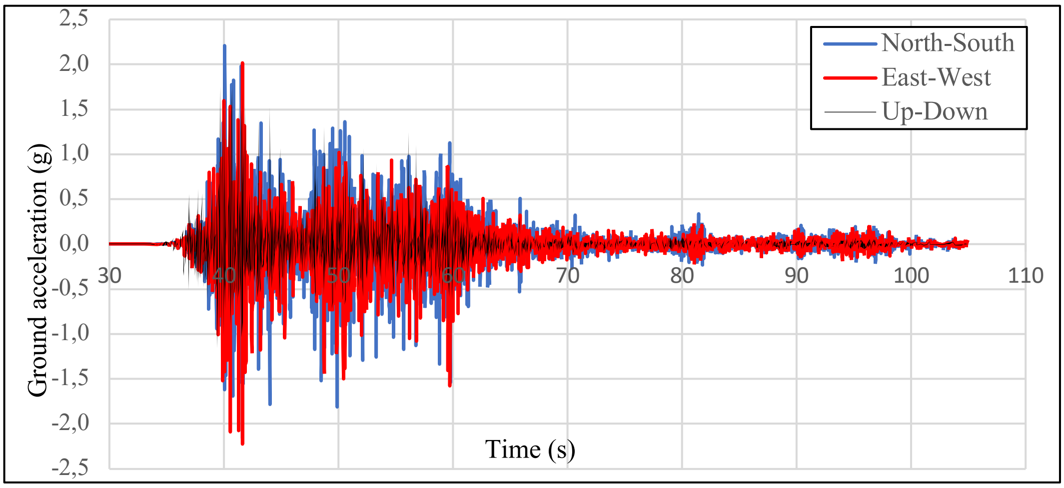

Figure 7. *Superimposed acceleration records from observation station 4614 during the Pazarcık Earthquake (7.7 M_W)*

As observed in Figure 7, the seismic energy was distributed significantly across all three dimensions. It should be noted that evaluating individual components separately may not fully represent the maximum earthquake demand on structures. Therefore, the resultant acceleration was calculated. In 17 instances between the 39th and 44th seconds of the record, the resultant acceleration magnitude exceeded 2.00 g (Table 6).

Table 6. *Acceleration records with vector sum (NS, EW, UD) of over 2.00 g in the Pazarcık Earthquake (7.7 M_W)*

Time (s)	Ground Acceleration (g)				
	North-South (NS)	East-West (EW)	Vertical (UD)	Horizontal Resultant (NS, EW)	3-D Resultant (NS, EW, UD)
39.64	1.04	-0.15	1.75	1.05	2.04
39.85	-0.77	-1.52	1.29	1.70	2.14
39.93	1.17	0.73	1.99	1.38	2.42
40.02	-1.62	-1.42	-0.23	2.15	2.17
40.06	1.02	1.15	1.48	1.54	2.14
40.07	2.21	0.35	0.44	2.24	2.28
40.54	-0.72	-1.73	1.62	1.87	2.48
40.55	-0.18	-2.09	-0.01	2.10	2.10
40.64	1.66	0.66	1.73	1.79	2.49
41.25	0.12	-1.27	1.57	1.27	2.02
41.26	0.07	-2.08	0.34	2.08	2.10
41.52	1.98	0.32	1.24	2.00	2.36
41.59	1.26	2.01	0.19	2.38	2.38
41.61	-2.16	-2.22	1.25	3.10	3.34
41.62	-1.54	-1.99	-0.60	2.52	2.59
41.84	-1.30	-1.43	0.54	1.93	2.01
43.99	-1.78	-0.50	0.79	1.85	2.01

Elastic Response Spectra

In structural engineering, elastic response spectra are essential tools used to determine the seismic loads acting on a system. Specifically, an Elastic Response Spectrum represents the maximum response of a single-degree-of-freedom (SDOF) system with a specific damping ratio (typically ξ = 5 %) to a given ground motion. While PGA represents the maximum discrete acceleration value of the ground motion; in contrast, the response spectrum illustrates how this motion translates into Spectral Acceleration (S_a) for structures with varying dynamic characteristics under the influence of ground motion by using free vibration mode shapes [28]. In this study, the response spectra derived from the February 6 records are given along with the Elastic Design Spectra (S_{ae}) defined in Turkish earthquake codes. Although a spectrum was given in the TEC-1975, a comparison cannot be made within the scope of this study since calculation details are not given; thus, the spectra in the 1998, 2007, and 2018 codes are examined. The use of past codes is necessitated by the presence of the existing building stock designed under these older regulations. To ensure a consistent comparison, the design spectral acceleration (S_{ae}) values were calculated based on the specific coordinates and soil conditions (V_{s30}) of the observation stations. The most unfavorable situation is assumed in the cases with uncertain data. The response spectra from the February 6 records were obtained directly from the AFAD webpage [27]. In creating modified acceleration response spectra from acceleration records, AFAD uses ITACA Strong-Motion Processing Service to process data according to a 5 % damping ratio (ξ) [29]. Accordingly, the raw accelerograms were subjected to standard signal processing procedures, including linear baseline correction and acausal band-pass filtering (Butterworth filter of order 2) typically within the 0.10-25.00 Hz frequency range. In this study, the specific horizontal component exhibiting the dominant spectral demand was selected for each record, rather than employing direction-independent averaging methods. This approach was adopted to preserve the maximum intensity of the seismic actions, specifically to capture the peak demands without smoothing out critical pulses. Similarly, elastic design spectra were determined also according to the 5% ξ from the codes. It should be noted that the response spectra are presented alongside the design spectra to highlight the exceptional severity of the ground motions for future research references, rather than to question the adequacy of the code provisions. The response spectra obtained from 4 events with the peak spectral acceleration $S_a(T)$ values over 1.00 g were selected and examined. The records used belong to the stations where the highest peak spectral acceleration values were recorded during the ground motions. Information about these events and the stations whose records were used is given in Table 7.

Table 7. *Event and station data of ground motions with $S_a(T)$>1.00 g [27]*

Earthquake						Observation station						
ID	Date /Time	Magnitude	Type	Depth (km)	Location	ID	Latitude	Longitude	V_{s30} (m/s)	Local Soil Class	PGA (g)	Peak $S_a(T)$ (g)
543428	06.02.2023 04:17	7.7	M_W	8.60	Pazarcık (Kahramanmaraş)	4614	37.485	37.298	541	ZC	2.22	7.51
543431	06.02.2023 04:28	6.6	M_W	6.20	Nurdağı (Gaziantep)	2712	37.184	36.733	599	ZC	0.46	1.33
543430	06.02.2023 04:36	5.7	M_L	11.19	İslahiye (Gaziantep)	2708	37.099	36.648	523	ZC	0.37	1.74
543593	06.02.2023 13:24	7.6	M_W	7.00	Elbistan (Kahramanmaraş)	4612	38.024	36.482	246	ZD	0.65	1.47

Earthquake Spectra in TEC-1998 and TEC-2007

The Spectral Acceleration Coefficient A(T) was first defined in TEC-1998 [22] as the Elastic Design Acceleration Spectrum divided by the gravitational acceleration g, for the 5 % ξ. Later in TEC-2007 [23], the Elastic Spectral Acceleration, $S_{ae}(T)$ was explicitly defined as the ordinate of the elastic design spectrum. The relationship is expressed as follows:

$$A(T)=A_0\, I\, S(T) \tag{14}$$

$$S_{ae}(T)=A(T)\, g \tag{15}$$

Here, A_0 represents the Effective Ground Acceleration Coefficient and I represents the Building Importance Factor. The values of A_0 vary by earthquake zone as summarized in Table 8 [22, 23].

Table 8. *Effective Ground Acceleration Coefficient A_0 [22, 23]*

Earthquake Zone	A_0
1	0.40
2	0.30
3	0.20
4	0.10

The Spectrum Coefficient S(T) is calculated according to Equations (6), (7), and (8) given in previous sections, depending on local soil conditions and building natural period T and Spectrum Characteristic Periods T_A and T_B. Additionally, Spectrum Characteristic Periods T_A and T_B are given in Table 9 depending on Local Soil Classes [22, 23].

Table 9. *Spectrum characteristic periods T_A and T_B [22, 23].*

Local Soil Class	T_A (second)	T_B (second)
Z1	0.10	0.30
Z2	0.15	0.40
Z3	0.15	0.60
Z4	0.20	0.90

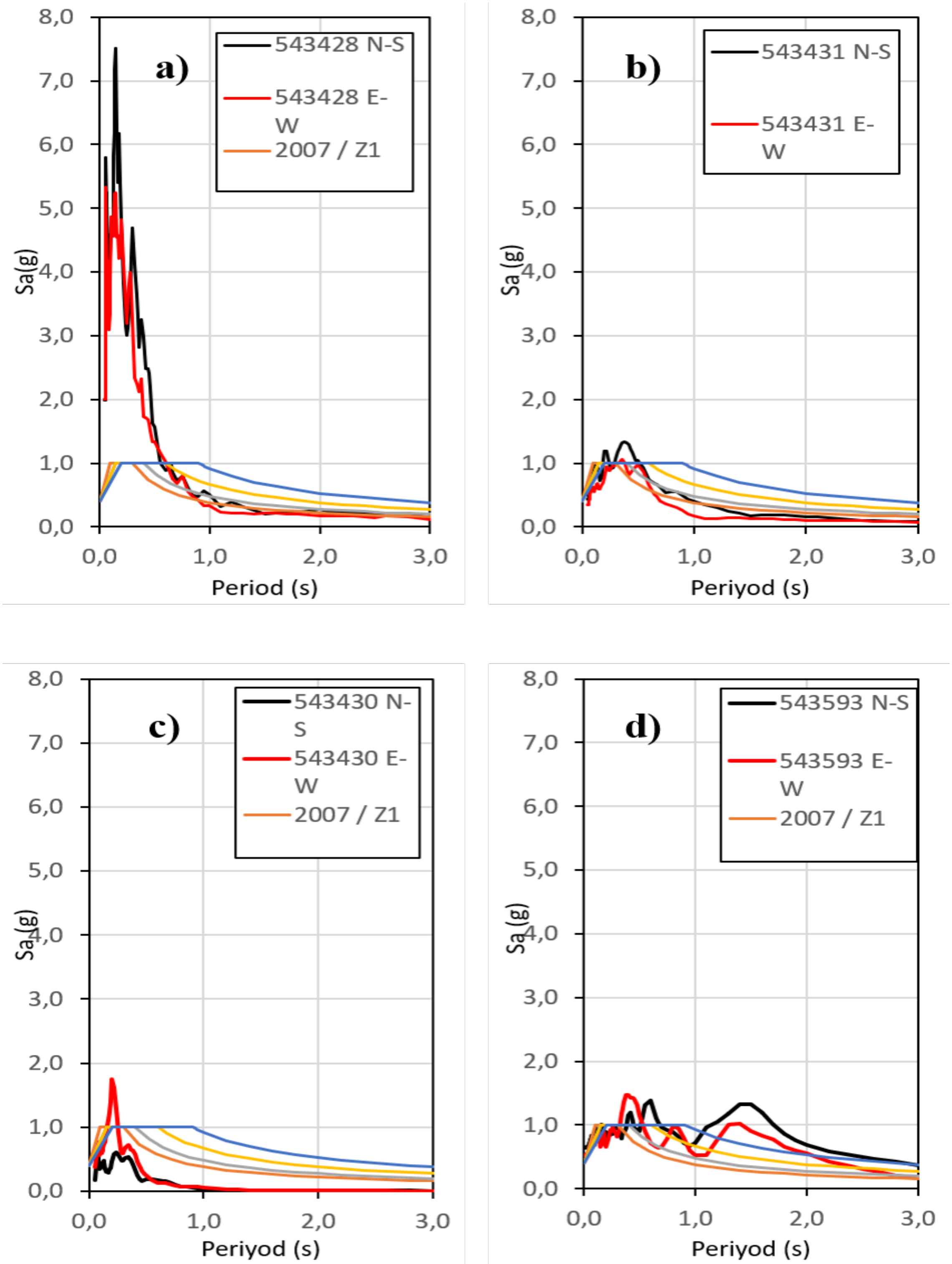

Figure 8. *Horizontal elastic design spectra (TEC-2007 - 5 % ξ) with response spectrum curves of events 543428 (a), 543431 (b), 543430 (c), 543593 (d)*

In this section, response spectra of four events (Table 7) for the critical directions are presented along with the Elastic Design Spectra determined in TEC-1998 and TEC-2007. In Figure 8, the curves labeled with earthquake IDs and direction information represent the computed spectral accelerations for those specific records, while the notation starting with 2007 represents the code-defined elastic design spectra for different soil conditions with 5 % ξ.

Earthquake Spectra in TBEC-2018

In TBEC-2018, data on earthquake ground motions to be taken as basis in the design of buildings under the influence of earthquakes are defined with four different ground motion levels [25]. The defined ground motion levels and their characteristics are summarized in Table 10.

Table 10. *Ground motion levels in TBEC-2018 [25]*

Ground Motion Level	Notation	Probability of Exceedance in 50 years	Repeat Period (Years)	Frequency of Occurrence	Naming
1	DD-1	2 %	2475	Very rare	Largest earthquake ground motion
2	DD-2	10 %	475	Rare	Standard design earthquake ground motion
3	DD-3	50 %	72	Often	Frequent earthquake ground motion
4	DD-4	68 %	43	Very often	Service Level Earthquake

Türkiye Earthquake Hazard Map is used for the four different ground motion levels in the design of structures in the country. The map is accessible online [30]. The ground motion data obtained here can be used in standard or site-specific earthquake hazard analyses based on Map Spectral Acceleration Coefficients and Local Ground Effect Coefficients for a 5 % damping ratio based on a specific earthquake ground motion level. From this, the horizontal elastic design spectrum is obtained for the observation locations. In TBEC-2018, design by Strength and Strain approaches have been defined along with normal and advanced performance targets to be applied to buildings for four different earthquake ground motion levels. Linear and non-linear calculation methods have been defined to be used in each approach. Since elastic design spectrum data determined by Türkiye Earthquake Hazard Maps is used in every method except the Time-History Analyses Method, the elastic design spectra were given along with the response spectra of the strong motion events used in this section. Unlike previous codes; since the elastic design spectra in the vertical direction are defined by this regulation, vertical response spectra were also used. The response spectra of the 4 events are examined and presented with the design spectra for the stations in Figure 9 in the horizontal direction and in Figure 10 in the vertical direction.

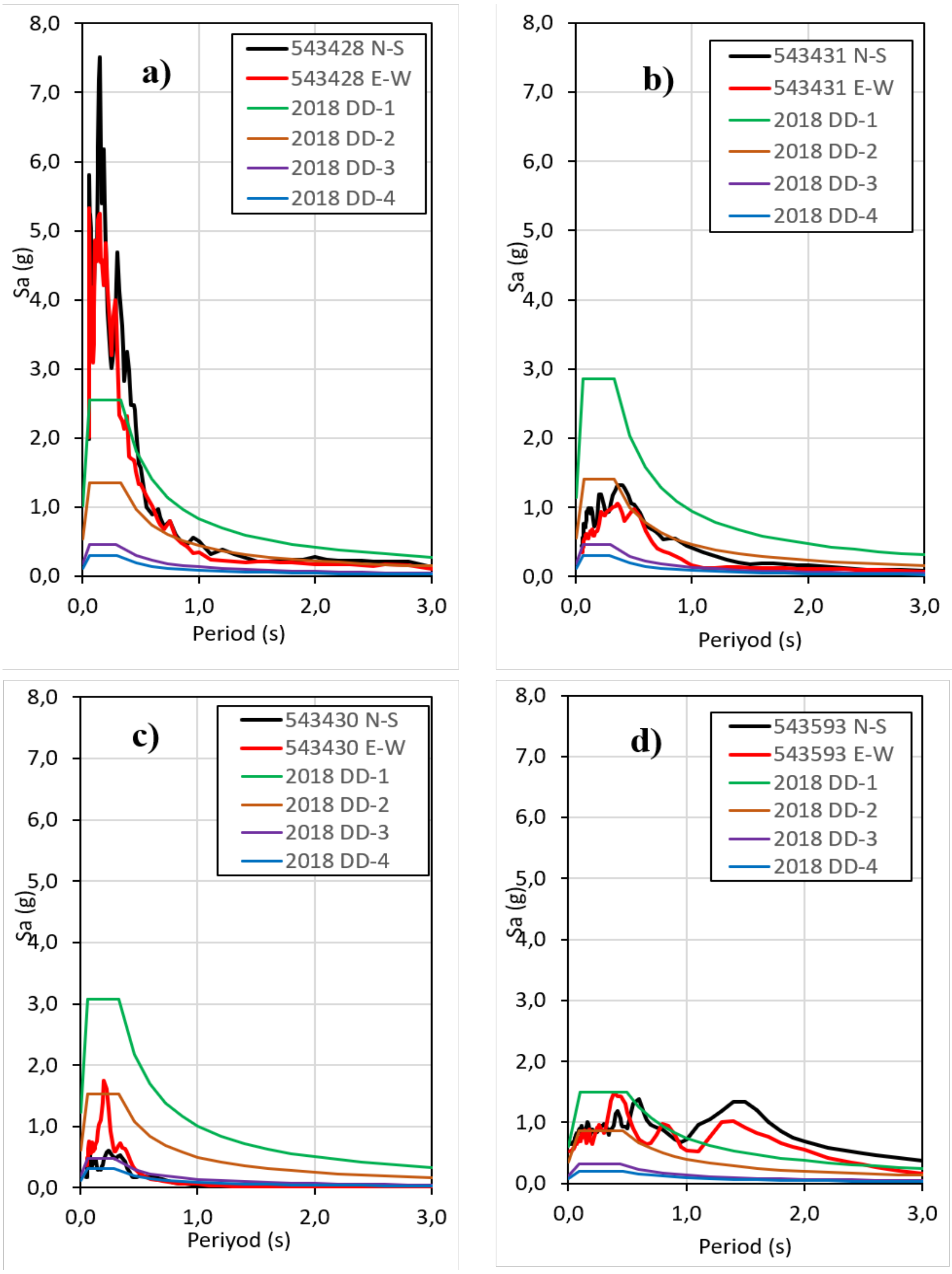

Figure 9. *Horizontal elastic design spectra (TBEC-2018 - 5 % ξ) with response spectrum curves of events 543428 (a), 543431 (b), 543430 (c), 543593 (d)*

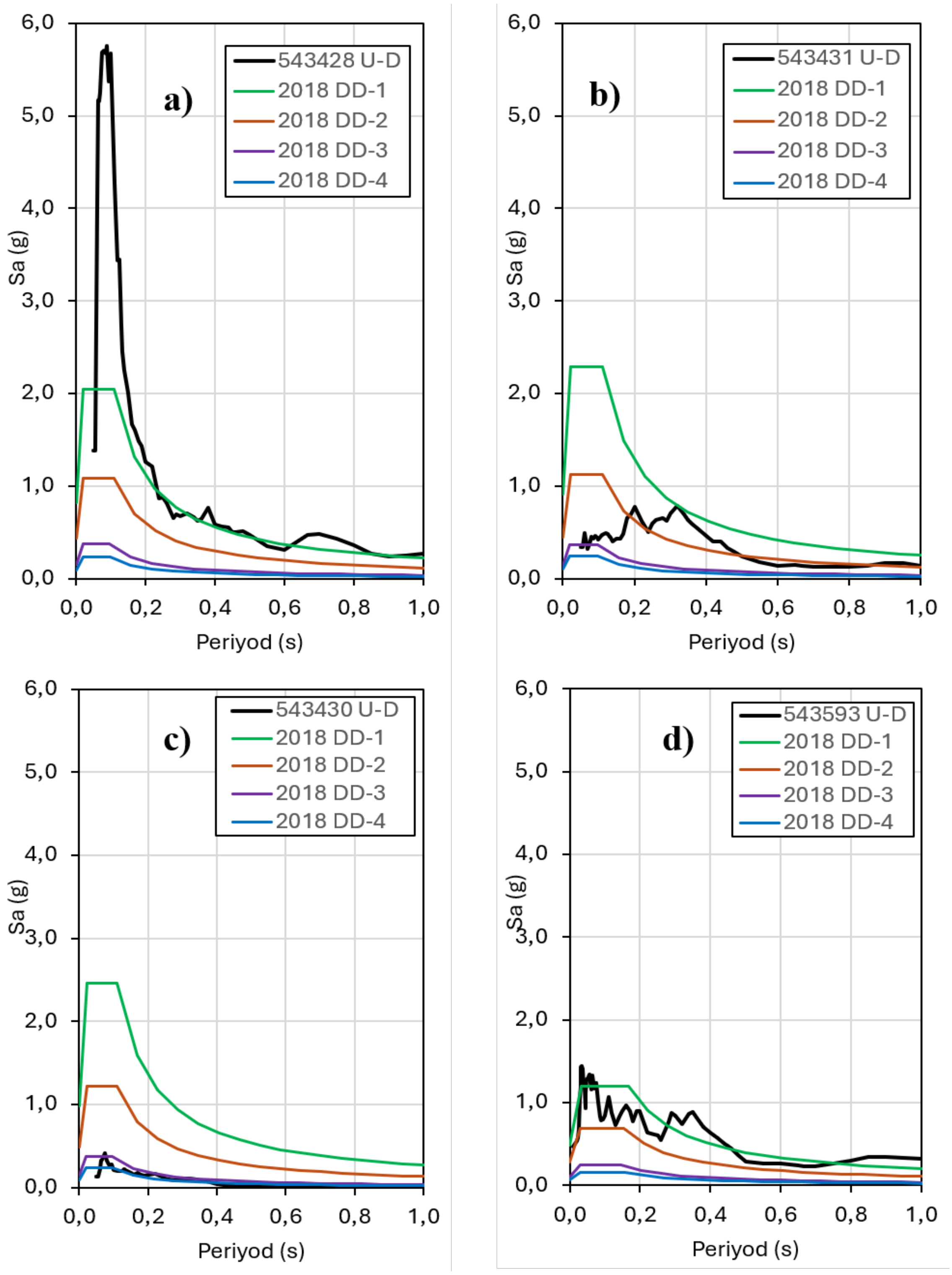

Figure 10. *Vertical elastic design spectra (TBEC-2018 - 5 % ξ) with response spectrum curves of events 543428 (a), 543431 (b), 543430 (c), 543593 (d)*

Limitations of PSHA and Epistemic Uncertainty

Although the design loads are defined with specific return periods (for example, 475 or 2475 years) through Probabilistic Seismic Hazard Analysis (PSHA) as incorporated in modern building codes, including the TBEC-2018, it is important to recognize the fundamental difference between probabilistic predictions and deterministic physical reality. The probabilistic prediction of seismic hazard, which

E-ISSN: 2564-7873

considers the aggregate potential of seismic sources and ground motions, is also prone to "epistemic uncertainty." This is defined as the uncertainty due to incomplete knowledge of fault geometry, slip rates, or maximum potential magnitude. This is very different from a deterministic approach, which considers a specific scenario, for example, a specific fault. It is also important to note that, unlike a deterministic prediction, which considers a specific scenario, probabilistic prediction "smoothes" the hazard over time and space. This means that, in the event of a rare "tail-end" event with complicated rupture characteristics, the ground motions can be substantially higher than those predicted probabilistically, which were based on historical data and models.

Results and Discussion

Within the scope of this study, the ground motion demands of the February 6 earthquakes are presented alongside the design seismic loads prescribed for reinforced concrete residential buildings by the Turkish earthquake codes. Not only the latest regulation but also the conditions in older codes were examined since the majority of the building stock in the field was constructed in the last 50 years. The results obtained are listed below.

A comparative analysis of the seismic codes reveals a trend: as regulations were updated over the last 50 years, the prescribed seismic design loads for the investigated region have gradually increased. Within the scope of this study, these demands are expressed as the Seismic Base Shear Coefficient (C_S), representing the ratio of the base shear force to the building's total weight. For the TEC-1975 [21], this coefficient was obtained from a static equivalent lateral force procedure, whereas for modern codes (TEC-1998 [22], 2007 [23], and TBEC-2018 [25]) corresponds to the Normalized Reduced Design Spectral Acceleration (S_{aR}/g). This coefficient serves as a unified metric to compare the equivalent static forces of older regulations with the reduced spectral demands of modern codes. To facilitate a robust assessment against the February 6 ground motions, Table 11 presents both the reduced design levels and the unreduced elastic demands (S_{ae}, where R = 1). The results indicate that the design seismic demand for the considered specific location has increased by approximately 70% from 1975 to 2018.

Table 11. *Evolution of seismic design coefficients and elastic demands*

Code	Calculation Method	Seismic Base Shear Coefficient (C_S or V_t/g)	Normalized Elastic Demand (S_{ae}/g)
TEC-1975	Equivalent Static Force	0.100	-
TEC-1998	Response Spectrum	0.125	1.000
TEC-2007	Response Spectrum	0.125	1.000
TBEC-2018	Response Spectrum	0.169	1.352

During the Pazarcık Earthquake (M_W 7.7), within a 20-second interval of the intense ground motion phase, Peak Ground Acceleration (PGA) values exceeding 1.00 g were recorded 53 times in the E-W direction, 99 times in the N-S direction, and 37 times in the vertical direction.

The ratio of values of peak accelerations in two orthogonal horizontal directions reached up to 97%, and the resultant acceleration (vector sum) reached a peak of 3.10 g at t = 41.61 s.

In the Pazarcık Earthquake (M_W 7.7), vertical acceleration components exceeding 1.00 g were observed, and a 3D resultant acceleration (3D vector sum) above 2.00 g occurred 17 times within only 5 seconds. The maximum 3D vector sum reached 3.34 g (including a 1.25 g vertical component) at the 41.61st second of the record.

For a 5 % damping ratio (ξ = 5 %), the maximum Elastic Spectral Acceleration (S_{ae}) values were calculated as 7.51 g in the horizontal direction and 5.76 g in the vertical direction from the records at station 4614 in the Pazarcık Earthquake (M_W 7.7).

The seismic demands of two separate events on the same day exceeded the Elastic Design Spectrum (S_{ae}) of the DD-1 level (the maximum considered earthquake) as defined in TBEC-2018 [25].

Undoubtedly, the peak ground motion demands imposed by the February 6 events vastly exceeded both the seismic base shear coefficients and elastic demands prescribed by the codes in Türkiye. However, this observation is not unique to the Turkish context; a comparative analysis of the historical evolution of global standards provides essential insight into these design values. In the context of PSHA, the ground motion levels defined in TBEC-2018 [25] conceptually align with these international standards. For instance, the standard design earthquake (DD-2) with a 475-year return period and the maximum considered earthquake (DD-1) with a 2475-year return period share the same probabilistic foundations as the Design Earthquake and Risk-Targeted Maximum Considered Earthquake frameworks outlined in FEMA [31] guidelines and ASCE 7 [32]. Similarly, Eurocode 8 [33] fundamentally relies on comparable probabilistic hazard assessments, traditionally anchoring its life safety requirement to a 475-year return period. Indeed, as in Türkiye, early-period regulations in the US (e.g., UBC-85 [34]) and Europe (e.g., Italian DM-1986 [35]) typically defined reduced seismic demand as a relatively low constant fraction of the structural weight (approximately 0.1 W). With the advent of modern guidelines and codes based on PSHA, such as FEMA P-1050 [31], ASCE 7 [36], and Eurocode 8 [37], these values have increased significantly. At present, for a typical reinforced concrete structure designed for high seismicity and high ductility, the codes in Türkiye [25] and the US [32] yield similar results due to the utilization of high response modification factors (up to R = 8). On the other hand, Eurocode 8 [33] adopts a more conservative stance regarding ductility capacity (around q = 4 to 4.5), thereby elevating the design base shear coefficient. Yet, even this enhanced design threshold implies design acceleration levels that are lower than the actual ground accelerations observed during the February 6 events. Nevertheless, these modern regulations signify the paradigm shift from deterministic coefficients to probabilistic hazard analyses, and hence the numerical progression of the nominal loads does not solely signify the actual advancement in structural safety. The true enhancement comes from the Capacity Design principle mandated by contemporary codes across all three regions. Coupled with stringent detailing requirements to preclude brittle failure and restricted inter-story drift limits, this approach maximizes the structure's energy dissipation capacity. Consequently, this evolution has substantially augmented both the actual safety levels and construction costs, extending far beyond the mere increase in nominal lateral loads.

It should be noted that the seismic design demands presented herein are based on specific assumptions regarding calculation parameters. A sensitivity analysis involving different soil classes (e.g., ZA to ZE) or ductility levels (e.g., R = 4 to R = 8) would naturally yield a broader range of design values. For example, according to TEC-2007 [23], the resulting seismic design coefficients (V_t/g) would theoretically range from approximately 0.01 to 0.25. When these design thresholds are evaluated considering the recorded PGA values (expressed in g) or normalized elastic spectral demands (S_{ae}/g) reaching 7.51, it is evident that the seismic demand remains significantly above the design limits, regardless of the variations in design parameters. It is crucial to emphasize that the exceedance of nominal design demands by actual seismic intensities does not inherently mean the current seismic code is inadequate. Seismic regulations must be evaluated as a holistic framework, in which design forces, safety factors, and detailing requirements function in unison to ensure structural performance. Furthermore, the structural integrity maintained by code-compliant buildings, coupled with the systemic construction and design errors summarized in Table 1, makes it evident that the observed destruction was not primarily a result of the magnitude of design seismic demands specified in the regulations. As discussed earlier, the safety of modern structures relies on energy dissipation through ductility rather than resisting the full elastic force. In an effort to elucidate the full extent of the seismic devastation from a holistic perspective, this study examines ground accelerations not only through their individual orthogonal components but also via their three-dimensional (3-D) vector magnitudes. While it is acknowledged that current structural design codes utilize specific combination rules for orthogonal effects (e.g., the 100/30 rule) rather than direct vector sums, the resultant peak ground acceleration is presented here to document the absolute severity of the seismic event. Consequently, these 3-D values are not intended for direct compliance comparison with seismic design coefficients but rather to serve as a comprehensive empirical record for future research and to highlight the intensity of the multi-directional shaking. In Türkiye, as in many other seismically active regions, the determination of seismic demands for structural design is conducted using elastic spectral acceleration (S_{ae}) values derived from PSHA. PSHA is based on the probability of exceedance of specific ground motion intensity levels over a given time horizon. Consequently, it is expected that recorded acceleration values during significant events may occasionally surpass the levels prescribed at the design stage [38]. This stems from the stochastic nature of ground-motion prediction models and the inherent variability of seismic events [39]. It should be emphasized that within the PSHA framework, ground motion intensity parameters for structural design are derived from historical seismic records. As such, the evaluation of past ground motion effects provides valuable insights for refining future hazard assessments. Therefore, the extreme values observed on February 6 necessitate a critical reassessment of PSHA parameters and practical design limits. To integrate these extreme seismic demands into future design practices, the following specific code revisions and methodological updates are strongly recommended:

Re-evaluation of Near-Fault Effects: The exceptionally high PGA (2.20 g) and spectral accelerations (7.51 g) indicate that current GMPEs used in PSHA may underestimate near-field pulse-like effects in this region. Future hazard maps should consider incorporating higher weighting for near-fault directivity and fling-step effects.

Vertical Ground Motion: Recording vertical ground accelerations over 1.00 g (reaching up to 1.99 g) simultaneously with extreme horizontal demands highlights a critical point. The V/H spectral ratios in our seismic design codes likely need a reassessment, especially for buildings in near-fault regions.

Scenario-Based Design: The DD-1 Elastic Design Spectrum (S_{ae}) was exceeded in two events just 9 hours apart. This shows that relying purely on probabilistic return periods may be insufficient. Therefore, adding deterministic scenario-based assessments to the code for critical structures near major fault lines would be a highly valuable step.

By integrating these “extreme” data points into the national seismic hazard database, the uncertainty can be reduced, leading to more robust design spectra in future revisions. This study elucidates the ground motion demands imposed by the 2023 ground motion events (Table 7) not only to document the scale of the disaster but also to provide the empirical basis required for refining PSHA parameters and design philosophies. By comparing these demands with other recent significant global events, the extent of the disaster can be more comprehensively understood (Table 12). Undoubtedly, with every disaster that occurs, all possible improvements will come to the fore.

Table 12. *Recent strong motions with high PGA values [27, 40, 41, 42]*

Event	Magnitude (M_w)	PGA/g	
		Max. Horizontal	**3-D Resultant**
2023 Pazarcık (Kahramanmaraş) [27]	7.7	2.20	3.34
2016 Kaikōura earthquake [40]	7.8	1.02	3.23
2011 Tōhoku earthquake and tsunami [41]	9.1	2.70	2.93
2008 Iwate-Miyagi earthquake [42]	7.2	1.13	4.10

On the other hand, by examining PGA values recorded in earthquakes and the spectral accelerations, the importance of dynamic effects is once again revealed. In the Pazarcık Earthquake (M_W 7.7), the peak horizontal PGA was 2.20 g, while the maximum peak spectral acceleration reached 7.51 g. Another interesting finding is that the maximum peak spectral acceleration value calculated in the Islahiye Earthquake (M_W 5.7) was higher than in the Elbistan Earthquake (M_W 7.6). This situation can be explained by the definition of earthquake magnitude, which represents total energy release. Therefore, it could be more appropriate to characterize seismic events not according to their magnitudes but according to their acceleration demands when evaluating from the civil engineering perspective, where the focus is on the acceleration transferred to the system.

Inherent Safety Margins, Redundancy, and Structural Overstrength

Another key factor is the role of inherent safety margins embedded in our codes. Those margins can be identified as; material safety factors, load combinations, redundancy, and structural overstrength. While it has been indicated that the recorded seismic demands clearly surpassed the design targets, the fact that many code-compliant buildings survived proves these mechanisms work. The reserve capacity of the buildings, driven by conservative material strengths, force redistribution, and ductile detailing, successfully absorbed the extreme demands. The survival of these structures after such devastation sends a clear message: current safety factors and detailing rules provide a solid defense. As a result, well-built structures can withstand forces that far exceed their nominal limits.

Conclusion

This study aimed to evaluate the seismic demands imposed on structures during the strong ground motions of February 6, 2023, in Kahramanmaraş and its vicinity. In post-earthquake studies, construction errors and material defects have come to the fore as the main causes of building damage, while the ground acceleration values recorded during ground motions have not been examined in detail. Rather than proposing a new design method, the primary contribution of this study is the systematic evaluation and interpretation of the measured acceleration records and calculated response spectra from the strong ground motions of February 6, 2023. To quantify the severity of the events, the measured seismic demands were compared against the design limits specified in the codes. Fundamentally, the code-specified values represent minimum design baselines. Consequently, the exceedance of these limits during an extreme event does not inherently imply the inadequacy of the codes or the underlying hazard analyses. In other words, it is not surprising for the demands generated by earthquakes to surpass the minimum design limits during an extreme event. Crucially, the observed spectral accelerations at near-fault stations exceeded not only the standard design earthquake level (DD-2) but also the Maximum Considered Earthquake level (DD-1), which corresponds to a 2475-year return period. Since modern seismic codes are founded on PSHA which defines design loads based on acceptable risk levels rather than deterministic guarantees against all possible physical extremes, the exceedance of these thresholds does not necessarily imply a methodological failure of the codes. Instead, it indicates that the region experienced a statistically extreme event. The magnitude of the recorded demands suggests that the ground motions likely challenged the tails of the GMPE distributions rather than merely deviating from median predictions. On the other hand, the maximum earthquake magnitude considered in PSHA is estimated by examining past seismic activities and empirical relationships based on fault dimensions. Moreover, the design spectra are obtained using empirical attenuation relationships, which are frequently determined using past earthquake data. From this perspective, both the prediction of maximum earthquake magnitude in PSHA and the estimation of ground accelerations produced by this maximum earthquake involve the examination of historical earthquake data. For this reason, the February 6 earthquakes, which recorded the largest acceleration values in the region ever, and the values of these demands must be carefully evaluated in the PSHA studies in the future. In this respect, February 6 is a critical day in terms of earthquake engineering. It is certain that the lessons learned after every major disaster will contribute to efforts to build safer and more durable structures in disaster-risk areas.

The extreme seismic demands of the February 6 events highlight the inherent epistemic uncertainties in PSHA and demonstrate that relying exclusively on probabilistic design loads may be insufficient in regions with complex fault interactions. In order to utilize these findings for the improvement of upcoming code revisions, a hybrid design framework is strongly recommended. Specifically, it is suggested that standard probabilistic models should be supplemented with site-specific, deterministic scenario-based design checks, particularly for vital structures located in near-fault zones and areas with significant local site effects. Furthermore, updating GMPEs in light of the recorded extreme data, promoting the transparent sharing of strong motion data, and formally incorporating performance-based design methodologies would be highly beneficial for mitigating future seismic risks.

Declarations

Acknowledgements:-

Funding/Financial Disclosure: The author has received no financial support for the research, authorship or publication of this study.

Ethics Committee Approval and Permissions: This study does not require ethics committee approval or any special permission.

Conflict of Interests: There is no conflict of interest or common interest.

Authors Contribution: The author has read and approved the final manuscript.

Artificial Intelligence (AI): The author declare that AI tools (Gemini) were used solely for language correction, translation, and readability enhancement during the preparation of this article. The author assume full responsibility for the originality, accuracy, and integrity of the entire text, including all AI-assisted language outputs.

References

[1] AFAD, Turkish Ministry of Interior Disaster and Emergency Management Presidency (2023). *Report of Pazarcık-Elbistan Kahramanmaraş (M_W: 7.7 – M_W: 7.6) Earthquakes on 6 February 2023*, Ankara, Türkiye (in Turkish).

[2] İnce, O. (2024). Structural damage assessment of reinforced concrete buildings in Adıyaman after Kahramanmaraş (Türkiye) Earthquakes on 6 February 2023. *Engineering Failure Analysis, 156*, 107799. https://doi.org/10.1016/j.engfailanal.2023.107799

[3] Ozturk, M., Arslan, M. H., & Korkmaz, H. H. (2023). Effect on RC buildings of 6 February 2023 Turkey earthquake doublets and new doctrines for seismic design. *Engineering Failure Analysis, 153,* 107521. https://doi.org/10.1016/j.engfailanal.2023.107521

[4] Altunsu, E., Güneş, O., Öztürk, S., Sorosh, S., Sarı, A., & Beeson, S. T. (2024). Investigating the structural damage in Hatay province after Kahramanmaraş-Türkiye earthquake sequences. *Engineering Failure Analysis, 157*, 107857. https://doi.org/10.1016/j.engfailanal.2023.107857

[5] Ivanov, M. L., & Chow, W. K. (2023). Structural damage observed in reinforced concrete buildings in Adiyaman during the 2023 Turkiye Kahramanmaras Earthquakes. *Structures, 58*, 105578. https://doi.org/10.1016/j.istruc.2023.105578

[6] Yıldız, Ö., & Kına, C. (2023). Geotechnical and Structural Investigations in Malatya Province after Kahramanmaraş Earthquake on February 6, 2023. *Bitlis Eren Üniversitesi Fen Bilimleri Dergisi, 12(3),* 686–703. https://doi.org/10.17798/bitlisfen.1282555

[7] Binici, B., Yakut, A., Kadas, K., Demirel, O., Akpinar, U., Canbolat, A., Yurtseven, F., Oztaskin, O., Aktas, S., & Canbay, E. (2023). Performance of RC buildings after Kahramanmaraş Earthquakes: lessons toward performance based design. *Earthquake Engineering and Engineering Vibration, 22(4)*, 883–894. https://doi.org/10.1007/s11803-023-2206-8

[8] Peker, O., & Altan, M. F. (2024). The effect of errors in structural system design on the structure damaged in 2023 Turkey earthquakes: A case study. *Engineering Failure Analysis, 157*, 107923. https://doi.org/10.1016/j.engfailanal.2023.107923

[9] Güleç, A. (2024). Kahramanmaraş depreminin yığma yapılar üzerindeki etkilerinin araştırılması. *Gazi Journal of Engineering Sciences, 9(3)*, 634–650. https://doi.org/10.30855/gmbd.0705094

[10] Kılıç, M. (2023) Investigation of the status of buildings in the risk reduction plans of 10 cities affected by the Kahramanmaraş earthquake and comparison with the situation after the earthquake. *Acil Yardım ve Afet Bilimi, 3(2),* 49-56.

[11] Çambay, E. (2023) Damage assessment of masonry structures in adıyaman province after Kahramanmaraş earthquakes (February 6, 2023), *Firat University Journal of Experimental and Computational Engineering, 2(3),* 114-123. https://doi: 10.5505/fujece.2023.47955

[12] Azak, T. E., & Ay, B. Ö. (2023). Characteristics of building stock in cities affected by the February 6, 2023 Kahramanmaraş earthquakes. *Jeoloji Muhendisligi Dergisi, 47(1)*, 47–66, (in Turkish). https://doi.org/10.24232/jmd.1294425

[13] Ünal, H., & Ergüler, Z. A. (2023). The effect of Kahramanmaraş earthquakes on engineering structures in Adıyaman-Gölbaşı settlement area and earthquake-soil interaction. *Yerbilimleri/ Earth Sciences, 44*, 202–221, (in Turkish). https://doi.org/10.17824/yerbilimleri.1313819

[14] Işık, N. S. (2023). Basen ve yakın fay etkilerinin deprem yer hareketi üzerindeki etkileri, Kahramanmaraş Pazarcık depremi antakya kayıtlarının değerlendirilmesi. *Jeoloji Mühendisliği Dergisi, 47(1)*, 67–86, (in Turkish). https://doi.org/10.24232/jmd.1299027

[15] Görüm, T., Tanyas, H., Karabacak, F., Yılmaz, A., Girgin, S., Allstadt, K. E., Süzen, M. L., & Burgi, P. (2023). Preliminary documentation of coseismic ground failure triggered by the February 6, 2023 Türkiye earthquake sequence. *Engineering Geology, 327*, 107315. https://doi.org/10.1016/j.enggeo.2023.107315

[16] Özkan, A., Solak, H. İ., Tiryakioğlu, İ., Şentürk, M. D., Aktuğ, B., Gezgin, C., Poyraz, F., Duman, H., Masson, F., Uslular, G., Yiğit, C. Ö., & Yavaşoğlu, H. H. (2023). Characterization of the co-seismic pattern and slip distribution of the February 06, 2023, Kahramanmaraş (Turkey) earthquakes (M_W 7.7 and M_W 7.6) with a dense GNSS network. *Tectonophysics, 866*, 230041. https://doi.org/10.1016/j.tecto.2023.230041

[17] Wu, F., Xie, J., An, Z., Lyu, C., Taymaz, T., Irmak, T. S., Li, X., Wen, Z., & Zhou, B. (2023). Pulse-like ground motion observed during the 6 February 2023 M_W 7.8 Pazarcık Earthquake (Kahramanmaraş, SE Türkiye). *Earthquake Science, 36(4)*, 328–339. https://doi.org/10.1016/j.eqs.2023.05.005

[18] Akinci, A., Dindar, A. A., Bal, I. E., Ertuncay, D., Smyrou, E., Cheloni, D. (2024). Characteristics of strong ground motions and structural damage patterns from the February 6th, 2023 Kahramanmaraş earthquakes, Türkiye. *Natural Hazards, 121*, 1209–1239. https://doi.org/10.1007/s11069-024-06856-y

[19] Sucuoglu, H., & Akkar, S. (2013). *Basic earthquake engineering: from seismology to analysis and design.* (Vol. 9783319010267). Springer International Publishing. https://doi.org/10.1007/978-3-319-01026-7H.

[20] Cansız, S. (2022). Türkiye'de kullanılan deprem yönetmeliklerinin özellikleri ve deprem hesabının değişimi. *Uluslararası Muhendislik Arastirma ve Gelistirme Dergisi, 14(1)*, 58–71, (in Turkish). https://doi.org/10.29137/umagd.948025

[21] TEC-1975. (1975). *Specification for structures to be built in disaster areas (ABYYHY-75)*, Ministry of Public Works and Settlement. Government of Republic of Türkiye; Ankara, Türkiye.

[22] TEC-1998. (1998). *Specification for structures to be built in disaster areas; Part III-earthquake disaster prevention (ABYYHY-98)*, Ministry of Public Works and Settlement, Government of Republic of Türkiye; Ankara, Türkiye.

[23] TEC-2007. (2007). *Regulations on structures constructed in disaster regions - Turkish Earthquake Code*, Ministry of Public Works and Settlement, Government of Republic of Türkiye; Ankara, Türkiye.

[24] Earthquake Zone Map (1996) Ministry of Public Works and Settlement, Government of Republic of Türkiye; Ankara, Türkiye.

[25] TBEC-2018. (2018). *Türkiye Building Earthquake Code*, Republic of Türkiye Ministry of Interior Disaster and Emergency Management Authority; Ankara, Türkiye.

[26] Earthquake Hazard Map (2018). Republic of Türkiye Ministry of Interior Disaster and Emergency Management Authority; Ankara, Türkiye.

[27] TADAS. (2020). *Turkish Accelerometric Database and Analysis System*, Republic of Türkiye Ministry of Interior Disaster and Emergency Management Presidency (AFAD). Available: https://tadas.afad.gov.tr/list-event

[28] Fan, X., Wang, K., & Xiao, S. (2018). Large-scale parallel computation for earthquake response spectrum analysis. *Engineering Computations, 35(2)*, 800–817. https://doi.org/10.1108/EC-08-2016-0294

[29] Puglia, R., Russo, E., Luzi, L., Felicetta, C., Pacor, F., & Lanzano, G. (2018). Strong-motion processing service: a tool to access and analyse earthquakes strong-motion waveforms. *Bulletin of Earthquake Engineering, 16*, 2641–2651. https://doi.org/10.1007/s10518-017

[30] TDTH. (2019). *Türkiye Earthquake Hazard Maps Interactive Web Application*, Republic of Türkiye Ministry of Interior Disaster and Emergency Management Presidency (AFAD). https://tdth.afad.gov.tr/TDTH/main.xhtml

[31] FEMA-P-1050-1. (2015). *NEHRP Recommended Seismic Provisions For New Buildings and Other Structures: Part 1, Provisions*, Building Seismic Safety Council (BSSC), Federal Emergency Management Agency, Washington, D.C., 2015.

[32] ASCE/SEI 7-22. (2022). *Minimum Design Loads and Associated Criteria for Buildings and Other Structures*, American Society of Civil Engineers (ASCE); Reston, Virginia, USA.

[33] EN 1998-1. (2004). *Eurocode 8: Design of structures for earthquake resistance - Part 1: General rules, seismic actions and rules for buildings*, European Committee for Standardization (CEN); Brussels, Belgium.

[34] UBC-85. (1985). *Uniform Building Code*, International Conference of Building Officials (ICBO); Whittier, California, USA.

[35] DM-1986. (1986). *Norme tecniche relative alle costruzioni sismiche (Decreto Ministeriale 24 Gennaio 1986)*, Ministero dei Lavori Pubblici, Gazzetta Ufficiale della Repubblica Italiana; Rome, Italy.

[36] ASCE 7-88. (1990). *Minimum Design Loads for Buildings and Other Structures*, American Society of Civil Engineers (ASCE); New York, USA.

[37] ENV 1998-1-1. (1994). *Eurocode 8: Design provisions for earthquake resistance of structures - Part 1-1: General rules - Seismic actions and general requirements for structures*, European Committee for Standardization (CEN); Brussels, Belgium.

[38] Iervolino, I. (2022). Ground-motion observations and probabilistic seismic hazard: frequently asked questions. *Seismological Research Letters, 93*, 2360–2366.

[39] Strasser, F. O., Bommer, J. J., Abrahamson, N. A. (2007). Truncation of the Distribution of Ground-Motion Residuals. *Journal of Seismology, 12(1)*, 79–105.

[40] Bradley, B. A., Razafindrakoto, H. N. T., Polak, V. (2017). Ground-motion observations from the 14 November 2016 M_W 7.8 Kaikoura, New Zealand, Earthquake and Insights from Broadband Simulations. *Seismological Research Letters, 88(3)*, 740–756.

[41] NIED, National Research Institute for Earth Science and Disaster Prevention (2011). *Off the Pacific Coast of Tohoku earthquake, Strong Ground Motion*. Japan.

[42] ERS, Earthquake Research Committee (2008). *Headquarters for Earthquake Research Promotion, The Iwate-Miyagi Nairiku Earthquake in 2008*. Japan.